



**HAL**  
open science

## **Pebbles Tracking Thanks to RFID LF Multi-Loops Inductively Coupled Reader**

Marjorie Grzeskowiak, Antoine Diet, Pape Sanoussy Diao, Stéphane Protat,  
Christophe Bourcier, Yann Le Bihan, Gaele Bazin Lissorgues

► **To cite this version:**

Marjorie Grzeskowiak, Antoine Diet, Pape Sanoussy Diao, Stéphane Protat, Christophe Bourcier, et al.. Pebbles Tracking Thanks to RFID LF Multi-Loops Inductively Coupled Reader. Progress In Electromagnetics Research C, 2014, 55, pp.129-137. 10.2528/PIERC14102403 . hal-02434422

**HAL Id: hal-02434422**

**<https://hal.science/hal-02434422>**

Submitted on 17 Jan 2020

**HAL** is a multi-disciplinary open access archive for the deposit and dissemination of scientific research documents, whether they are published or not. The documents may come from teaching and research institutions in France or abroad, or from public or private research centers.

L'archive ouverte pluridisciplinaire **HAL**, est destinée au dépôt et à la diffusion de documents scientifiques de niveau recherche, publiés ou non, émanant des établissements d'enseignement et de recherche français ou étrangers, des laboratoires publics ou privés.

## Pebbles Tracking Thanks to RFID LF Multi-Loops Inductively Coupled Reader

Marjorie Grzeskowiak<sup>1, \*</sup>, Antoine Diet<sup>2</sup>, Pape S. Diao<sup>1</sup>, Stephane Protat<sup>1</sup>,  
Christophe Bourcier<sup>1</sup>, Yann Le Bihan<sup>2</sup>, and Gaelle Lissorgues<sup>3</sup>

**Abstract**—The Radio Frequency Identification (RFID) Low Frequency (LF) serial loops structure is proposed to improve TAGs detection when a TAG coil-antenna rotates by any angle, due to the tagged pebble moving. The detection zones of two types of TAGs (the token and glass TAG) and two types of reader coils, in function of the TAG size, TAG orientation and shape of the reader coils are tested. The effect of the proposed multi-coil inductively coupled is confirmed by measurement using a commercial LF RFID system.

### 1. INTRODUCTION

To evaluate the position (i.e., the TAG position into the plane of the reader antenna) whatever the TAG orientation (i.e., the angle between the TAG and the plane of the reader antenna), UHF-RFID systems are generally used, but these systems are not even effective when the media become water. On the other hand, the reading range of LF-RFID technology is very short but can penetrate dielectric material, like water. For tracking bed-load transport in gravel-bed rivers or seas [1], Passive Integrated Transponders (PIT TAG) are inserted in the pebbles or stacked on the pebbles. The effect of the pebbles and water immersion is supposed to be minor for the TAG detection at the LF frequencies, so seems to be effective for the pebbles tracking. However, the TAG orientation and position versus the reader coil can disrupt the TAG detection and has to be studied.

The detection distance between a reader and a TAG for Near-field Magnetic Induction Link depends on the orientation between the coils. The coils inductances are generally determined by empirical formulas. The mutual inductance between the consecutive turns of the loop can be accurately calculated by the complete elliptic integrals, and the calculus of the mutual inductance of two loops can be realized versus the position and orientation of the coils [2]. The mutual inductance between the reader coil and the TAG coil can be evaluated theoretically in the TAG parallel and perpendicular configuration. The loops can be associated in serial or parallel configuration in forward and reverse sense to modify the B-field distribution and assure better energy transfer efficiency between the loops. Multi-loops arrays, by splitting the loop in small loops, can improve the null-zone avoidance using the diversity combining of loop [3, 4] or by including several forward and reverse loops can provide free TAG positioning [5, 6] and orientation [7, 8].

This paper presents the token and glass TAGs detection with the respect of their orientation versus the reader by a single octagonal coil as well as an octagonal coil array on the same surface area in the air media. The multi-loop structure is not verified theoretically, or by simulation but the working principle for the reverse structure and the size of the loops is exposed to argue the scientific approach. The performance of the proposed structure is verified by measurement results. Both perpendicular and

---

*Received 24 October 2014, Accepted 4 December 2014, Scheduled 18 December 2014*

\* Corresponding author: Marjorie Grzeskowiak (marjorie.grzeskowiak@u-pem.fr).

<sup>1</sup> Université Paris-Est, ESYCOM (EA 2552), UPEMLV, ESIEE-Paris, CNAM, F-77454 Marne-la-Vallée, France. <sup>2</sup> LGEP UMR 8507, Rue Joliot Curie, Plateau du Moulon, F-91192 Gif Sur Yvette, France. <sup>3</sup> Université Paris-Est, ESYCOM, UPEMLV, ESIEE-Paris, CNAM, Cité Descartes, BP99, 93162 Noisy le Grand, France.

parallel TAG orientations were tested. Perpendicular and parallel orientations were chosen because they correspond to the worst and best detections for the token TAG, and it is the opposite case for the glass TAG. Since the reader for the pebbles tracking is towed by a boat, some different parts of the reader coil flow over the TAG, so serial loops, able to detect both parallel and perpendicular orientations, seem better than a coil, allowing any null of detection for only one orientation. The null of detection, in considering the both orientations, is decreased for the 10 coils structure, for the token TAG and the glass TAG.

## 2. MUTUAL INDUCTANCE CONSIDERATIONS

To study theoretically the magnetic coupling, the mutual inductance between the reader and the TAG coils is calculated. The TAG coil is represented by a circular loop of 1 cm diameter, and the reader by a squared loop of  $L$  length. The squared loop can define a surface on which the magnetic flux is integrated easily [9, 10]. As the mutual inductance is reciprocal, the circular loop is considered generating the  $B$ -field by the  $I_1$  current circulation on the loop. The magnetic field ( $B_r$ ,  $B_\theta$ ,  $B_y$ ) evaluated in the  $(x, y, z)$  position, generated by a circular loop of  $R$  radius positioned in the  $(xOz)$  plane (Figure 1), centered in  $(0, 0, 0)$  is expressed in equation (1):

$$\left\{ \begin{array}{l} B_r = \frac{I\mu_0 y}{2\pi [(R+r)^2 + y^2]^{1/2}} r \left[ \frac{R^2 + r^2 + y^2}{[(R-r)^2 + y^2]} E(k) - K(k) \right] \\ B_\theta = 0 \\ B_y = \frac{I\mu_0}{2\pi [(R+r)^2 + y^2]^{1/2}} r \left[ \frac{R^2 - r^2 - y^2}{[(R-r)^2 + y^2]} E(k) - K(k) \right] \\ k^2 = \frac{4Rr}{[(R+r)^2 + y^2]} \end{array} \right. \quad (1)$$

where  $r$  corresponds to the distance between the center of the circular loop and the functions  $K(k)$  and  $E(k)$  to the complete elliptic integral of first and second kinds, respectively. By discretizing equation (1), with a 500  $\mu\text{m}$  space the mutual inductance can be calculated with the MATLAB software and provides the following simulated part.

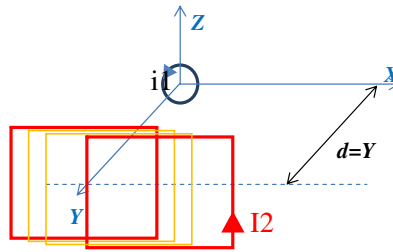


**Figure 1.** Squared loop for the reader coil in the TAG parallel configuration.

### 2.1. Size Constraints Between the Reader and TAG Coils in the Parallel Configuration

The size of the RFID reader, to perform a sufficient volume of detection, has to be large enough, but the magnetic coupling between the reader and the TAG coils can be reduced due to the size constraints between the both coils.

When the coils are co-axially parallel and spaced from a distance of  $d$ , as seen in Figure 2, the mutual inductance between the coils is reported versus the length of the squared loop, for different distances  $d$ .

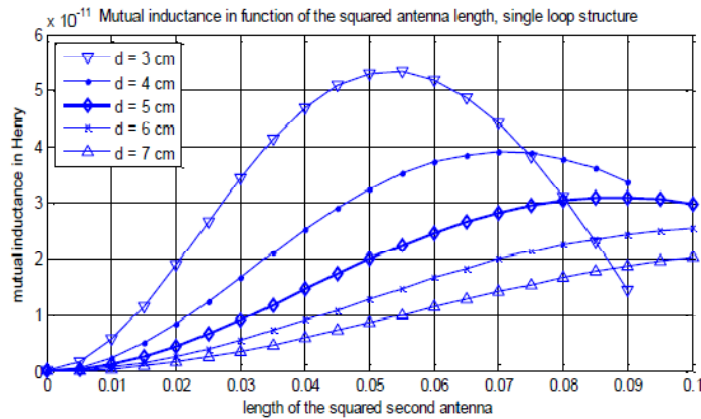


**Figure 2.** Mutual inductance versus the length of the squared loop in the TAG parallel configuration.

The mutual inductance (noted  $M$ ) depends on the length of the squared loop for a given distance. When the distance increases, the length of the squared loop has to be increased to optimize the mutual inductance. However, in considering the  $M$  optimum value for each  $d$ , the maximum value decreases when the length  $L$  increases. In the pebbles tracking, where a reader coil is necessarily large to prospect a great volume, and to favor the magnetic coupling with a small TAG (1 cm diameter in the simulated part), a structure constituted of small loops seems a good alternative. The diameter of these small loops can optimize the magnetic coupling at a read range distance for the TAG given diameter.

### 2.2. Improvement of the Mutual Inductance in the Reverse Structure in the Normal Configuration

Furthermore, the TAG loop can be rotated versus the reader coil plane, so decreases the magnetic coupling [11]. To study theoretically the magnetic coupling, the mutual inductance between the reader and the TAG coils is calculated: two serial loops, whose current circulates in the same sense (forward loops) or in the opposite sense (reverse loops), are coupled with the TAG coil: the maximum value of the mutual inductance indicates the optimization of the magnetic coupling.

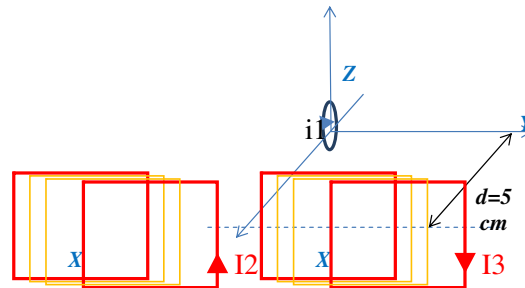


**Figure 3.** 2-reverse squared loops for the reader coil in the TAG normal configuration.

We study the worst case, when the TAG coil is oriented normally, in the  $(x0z)$  plane with the reader coil  $(y0z)$  plane, as seen in Figure 3. The TAG center is moved from 0 to 10 cm in the  $y$ -axis and is 5 cm away from the center of the two-loop reader coil in  $x$ -axis, whose centers are spaced 10 cm, and the length  $L$  is equal to 7.5 cm for each squared loop. We compare the reverse configuration where the  $I_2$  and  $I_3$  currents are out-of-phase, noted in/out-of-phase orthogonal loop on the Figure 4, with the single squared loop, noted orthogonal single loop.

For the single squared loop, the optimum value of the mutual inductance is obtained for a  $dy$  misalignment of 3.5 cm, i.e., under the wire, which generates a magnetic field around the wire. This

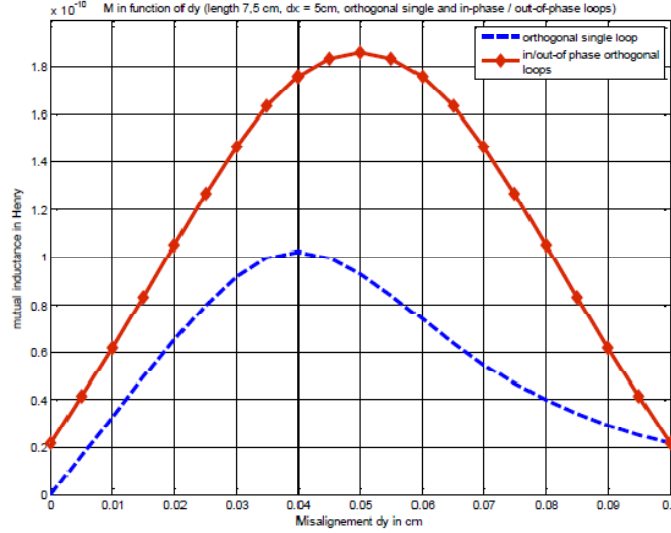


**Figure 4.** Mutual inductance versus the  $dy$  misalignment in the TAG normal configuration.

value is almost doubled by using the reverse configuration. The reverse multi-loop reader appears like a possible answer to detect TAG in the worst case, i.e., the normal configuration.

Considering the obtained theoretical results on the mutual inductance, valuable when the shape of the reader loop is circular or hexagonal, a demonstrator has been realized. With powerful numerical methods, such as Finite Element Method (FEM), it is possible to calculate accurately the mutual inductance. However, the electromagnetic solver is commonly used for radiating propagation. In the present case, the study is no-radiating, and the wavelength is very high in comparison with the coil, which is electrically small, so the computation time is generally long. We focused in the following part on the multi-loop design by empirical formulas and experimental studies.

### 3. DESIGN OF A CONVENTIONAL OCTAGONAL LOOP

Figure 5(a) represents a conventional single octagonal loop. The size of the PVC plate, on which the octagonal loop is realized, is 300 mm  $\times$  400 mm. The 28-turn coil is wound with copper enamel wire of 11.25  $\mu$ m section radius. The number of turns was first calculated equal to 25 by the empirical formula (2) and then modified to 28 when the fabricated coil is realized: a 700  $\mu$ H inductance value  $L$  is necessary to realize a resonant circuit at 125 kHz (3) with Ib-technology Micro-RWD reader (i.e., The capacitance value  $C$  is equal to 2.45 nF). The optimization of turn number allows avoiding the addition of another capacitance; the 2.45 nF capacitor has been integrated in the commercial reader system.

$$N = (\text{approx})^{1,9} \sqrt{\frac{L}{2 \cdot A \cdot \ln(A/D)}} \quad (2)$$

$$f_r = \frac{1}{2\pi\sqrt{LC}} \quad (3)$$

### 4. DESIGN OF THE 10-COIL ARRAY

Figure 5(b) shows the proposed structure. Each hexagonal coil is wound with copper enamel wire of 11.25  $\mu$ m section radius, has a circumference of 18 cm and presents an inductance value of 70  $\mu$ H by (1) with a turn number of 20. The circumference of 18 cm for each loop is a compromise value to detect TAG of diameter of 30 mm and 3.15 mm respectively for token TAG and glass TAG with the same structure. This circumference could be optimized for one type of TAG at a given read range, as previously exposed. Two 21 and 22-turn coils, whose opposite wires are separated from 40 mm, electrically serial connected

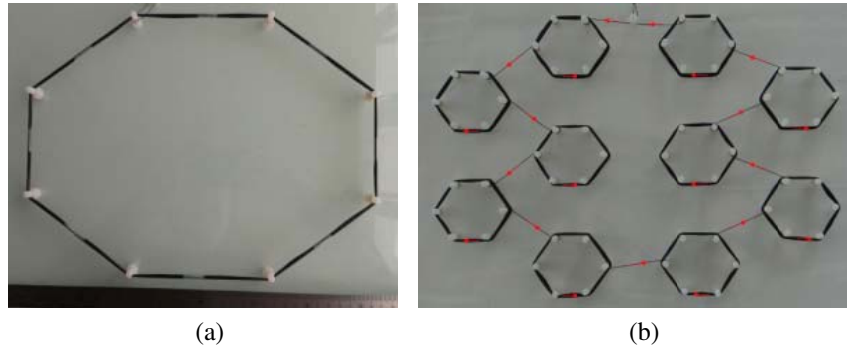


**Figure 5.** Photographs of the fabricated coils (a) single octagonal coil, (b) a 10-coil array.

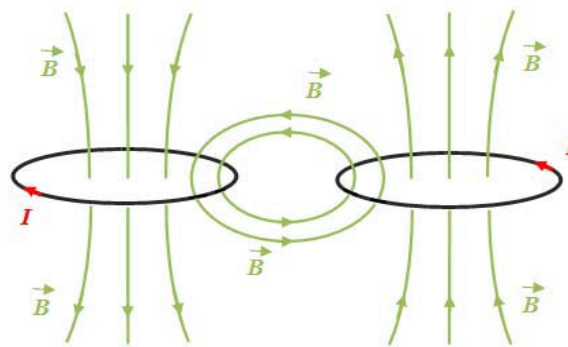


**Figure 6.** Loops in reverse sense and magnetic field lines.

in reverse current (Figure 6), improve the obtained inductance value of  $4.74 \mu\text{H}$  (and in forward current of  $2.44 \mu\text{H}$ ), due to the mutual inductance and also allows the TAG detection in a normal orientation. The number of loops, with 18 cm circumference, is optimized in the function of available surface. The hexagonal shape of the multi-loop allows easier realization than for a circular shape, which is used in the pebbles tracking’s systems [12].

To verify the TAG immunity of the angular misalignment effect, the investigated proposed structure is assumed to have the same effective area, for the results to be valid, for a combination of forward and reverse 26 and 27-turn loops. (Figure 5(b)). It is thought that the magnetic field distributions of the proposed structure are even more than a conventional coil.

### 5. EXPERIMENTS

The calculated electrical specifications of both the reader loops are reported in Table 1. The impedance (inductance and resistance) measures are carried out with the Rhode Schwarz ZNB8 VNA. The quality factor, deducted by formula (4), is relative to the energy transfer and inversely proportional to 3 dB

**Table 1.** Optimized geometries of coils and calculated specifications of the reader coil.

	Single octagonal coil	10-coil array
Inductance ( $\mu\text{H}$ )	663	661
Resistance ( $\Omega$ )	11.2	17.5
Number of turn	28	26 and 27
$Q_1$	46.5	29.7

bandwidth  $\delta F$ , necessary to high data transfer.

$$Q = \frac{L\omega}{R} \quad (4)$$

To obtain structures with the same quality factor, a serial resistance can be added for the single octagonal coil: in this case, the reduction of the energy transfer efficiency causes the decrease of the magnetic field flux and the deterioration of the TAG detection. So, a serial resistance has not been added to obtain the single coil with the same  $Q$  factor of the multi-loop reader: if the  $Q$  is lower for the single coil, the reader is unable to detect a glass TAG at 1 cm distance from the reader coil, and we cannot compare the both reader structures

The structures, whose electrical characteristics are reported on the Table 1, are associated with the Ib-technology Micro-RWD reader, token TAG (30 mm diameter) and glass TAG (3.15 mm  $\times$  13.3 mm), whose ASK (amplitude Shift Modulation) carrier frequency is 125 kHz. The receiving TAG coil moves along the  $X$ -axis from 0 mm to 400 mm and along the  $Y$ -axis from 0 mm to 300 mm at the separation distance  $Z$  equal respectively to 4 cm and 1 cm away from the reader coil, for the token TAG and glass TAG. The distance corresponds to the distance between the top of the reader coil wires and the TAG bottom and centre. However, if the distance is short, the coupling factor between the reader and TAG resonant coils increases. This phenomenon causes the separation of the resonant frequencies and degrades the efficiency and the TAG detection [13]. The choice of distance has to assure a weak coupling between the reader and TAG coils. To enhance the communication distance, the diameter of the reader loops can be optimized, as seen in the theoretical part concerning the mutual inductance, but it is limited. An alternative is to increase the current and so improve the  $H$ -field level, but in order to support greater current, the radius section of the wire will be increased. Moreover, the current/power is not limited by the electromagnetic emission regulations in the  $B$ -field generation, because the magnetic coupling is a no-radiation phenomenon. The Micro RWD is designed to restrict the pulse current less than 200 mA pp with a peak voltage up to 200 v and optimal coil ( $L = 700 \mu\text{H}$  and  $Q$  around 20). Both perpendicular and parallel TAG orientations (Figure 7) were tested, i.e., TAGs were oriented perpendicularly (TAG orientation  $\alpha = 90^\circ$ ) or parallel (TAG orientation  $\alpha = 0^\circ$ ) to the antenna plane ( $X, Y$ ). The actual coil structure in the used commercial TAGs cannot be seen without destroying the TAGs: it is just important to note a radius ratio of almost 10 between the token TAG and the glass TAG.

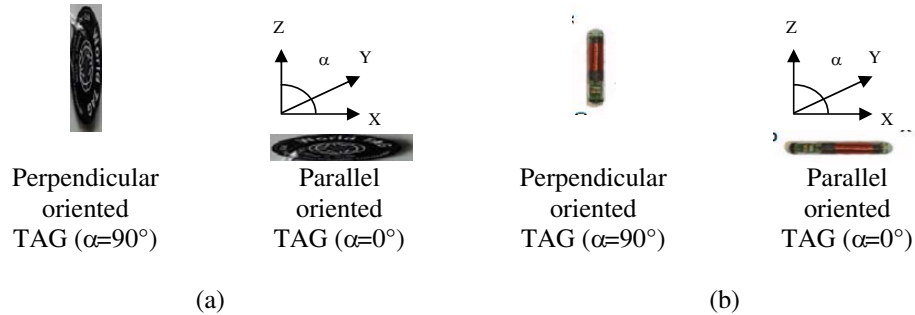


**Figure 7.** TAG orientation in ( $X, Y, Z$ ) coordinate system (a) token TAG, (b) glass TAG.

The data of TAG detection are curved in Figure 8 and in Figure 9. The white color indicates the detection and the black the null-detection for the token TAG (Figure 8) and for the glass TAG (Figure 9).

In a 10-coil configuration, for the token TAG (Figure 8(a)), the prototype provides a proportional surface area of 57% when the TAGs coil is parallel to the structure and of 81% for normal configuration for a separation distance of 4 cm, while in a single coil configuration, the surface area is increased from 57% to 86% for a TAG parallel position versus the reader, and reduced from 81% to 40% for the normal configuration for the same separation distance.

For a glass TAG, the surface area, equal respectively to 70% and 46% in parallel and perpendicular orientations for 10 coils structure, becomes equivalent to 39% and 79% with the single coil for a separation distance of 1 cm.

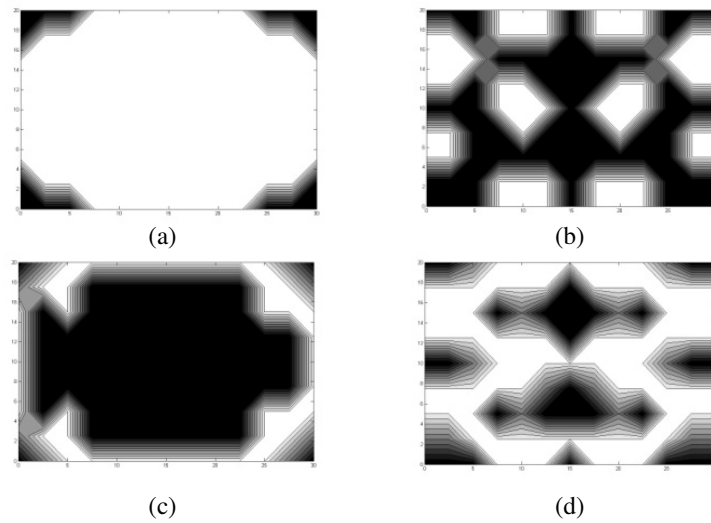


**Figure 8.** Detection in open air conditions for the both coils with token TAG in parallel ( $\alpha = 0^\circ$ ) and perpendicular ( $\alpha = 90^\circ$ ) orientation. (a) Parallel orientation for the single coil. (b) Parallel orientation for the 10 coils structure. (c) Perpendicular orientation for the single coil. (d) Perpendicular orientation for the 10 coils structure.

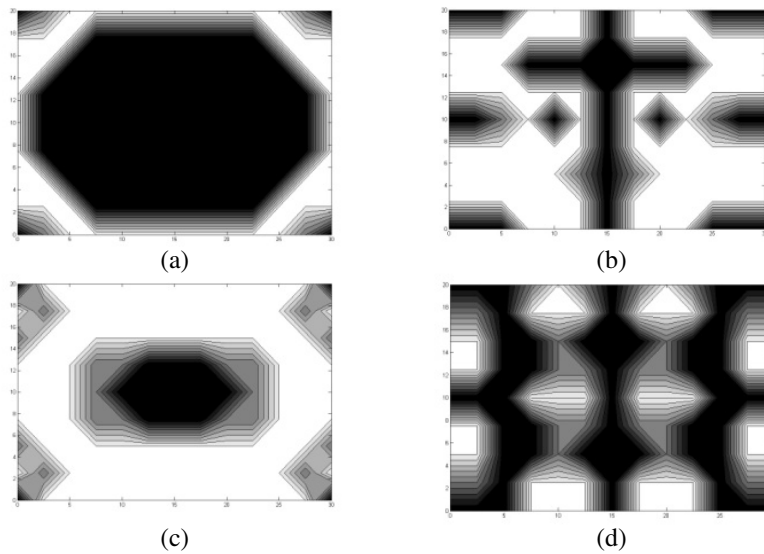


**Figure 9.** Detection in open air conditions for the both coils with glass TAG in parallel ( $\alpha = 0^\circ$ ) and perpendicular ( $\alpha = 90^\circ$ ) orientation. (a) Parallel orientation for the single coil. (b) Parallel orientation for the 10 coils structure. (c) Perpendicular orientation for the single coil. (d) Perpendicular orientation for the 10 coils structure.

In the theoretical part concerning the mutual inductance, we observe that the diameter of each multi-loop can optimize the magnetic coupling at a read range distance for the TAG given diameter. In our study, we prefer to use a unique multi-loop structure for each TAG, and we need to compare it with a single coil. We remember that a radius ratio between the token TAG and the glass TAG is around 10. So, we have to modify the distance from the reader coil, to assure a sufficient magnetic coupling. For the glass TAG, at a 4 cm distance from the single coil, we obtain a null of detection for the parallel and normal configurations. Furthermore, at 1 cm distance for a token TAG, in the multi-loop structure, the strong coupling between the reader and TAG resonant coils causes the separation of the resonant

frequencies of each coil and degrades the efficiency and the TAG detection. To conclude, two tags were tested at different distances from the reader coil to compare the multi-loop structure with the single coil.

As the position of RFID TAG is randomly varied in the space and time, it is more interesting and fruitful to provide a reader coil which can detect different positions with some nulls of detection rather than an antenna which does not present any null of detection, but for only one dedicated position of the tag (parallel for instance), and is almost unable to detect the tag in another position (perpendicular for instance). Some nulls of detection for the 10-coil structure, considering both orientations, are reduced in comparison with the single coil, for the token TAG and the glass TAG.

A decreasing of the quality factor for the single coil structure (Figure 5(a)) exhibits the best performances of the 10 serial loops structure (Figure 5(b)) to limit the null of detection. Token TAGs seem much more effective than glass TAGs for the realized structures, but the glass TAGs detection improves more with the multi-loops structure, in comparison with the single coil. It is seen that the proposed 10-coil array features a more robust misalignment and improves the global detection area surface for the parallel and perpendicular orientation.

## 6. CONCLUSION

The fundamental question examined in this paper is whether the coils are immune to the angular in the respect of the angular misalignment effects. Optimum reader coil geometry for LF TAG with respect to read angular displacement and operating frequency of the RFID systems is proposed. A theoretical mutual inductance, for forward and reverse of both loops in the reader structure, is calculated between the reader and the TAG to illustrate the advantage of the reverse loops to detect TAG in perpendicular orientation and the impact of the size constraints between both coils. In a 10-coil configuration, a prototype, which includes 10 forward and reverse coils, provides freer positioning and orientation to a smaller TAG coil. The performance of the proposed structure is verified by measurement results and improves the coupling efficiency between the reader and the TAG, incorporating misalignment effects, in comparison with a single loop with the same electrical and size specifications (inductance and area).

In future works, with the prototype, it should be investigated if the multi-loop structures may modify the anti-collision capability when multiple tags are presented in the field of view of the RFID reader. If not, the choice of the TAGs and of the reader should meet these specifications

The presented technology can be applied to other systems, which need to detect a TAG, arbitrarily oriented. For a dissipative medium, the LF is recommended due to its penetration in the dielectric, but for a non-dissipative dielectric, the HF can be favored, because of the larger bandwidth of the system. For instance, the working principle can be utilized to realize a belt or coverage on the human body abdomen to detect an ingestible capsule in the small intestine: the human body is a dissipative medium. The small intestine is located 5 cm away from the skin, and the ingestible capsule is arbitrarily oriented. The array can be scalable in frequency (for instance 13.56 MHz). For HF systems, the working principle can be used, but in this case, the inductance value is smaller (for instance a inductance value of 1.2  $\mu\text{H}$  is recommended with the Ib-technology Micro-RWD reader), and the loop cannot be connected in serial configuration: a parallel configuration should be studied for the HF systems, with loops switching, if the reader surface has to be large enough. With the progress of the miniaturization in the cleaning room, the working principle should be applicable in the tag coils as well. But perhaps a high cost could limit this possibility...

## REFERENCES

1. Benelli, G., D. Bertoni, and G. Sarti, "An analysis on the use of LF RFID for the tracking of different typologies of pebbles on beaches," *IEEE RFID-TA*, 426–431, 2011.
2. Babic, S. I., F. Sirois, and C. Akyel, "Validity check of mutual inductance formulas for circular filaments with lateral and angular misalignments," *Progress In Electromagnetics Research M*, Vol. 8, 15–26, 2009.

3. Hirayama, H., Y. Satake, N. Kikuma, and K. Sakakibara, "A new scheme to avoid null zone for HF band RFID with diversity combining of loop antennas," *IEICE transactions on Communications*, Vol. 93, 2666–2669, 2010.
4. Wang, K., A. Diet, S. A. Chakra, C. Conessa, M. Grzeskowiak, T. Bouaziz, S. Protat, D. Delcroix, L. Rousseau, G. Lissorgues, and A. Joisel, "Detecting range and coupling coefficient tradeoff with a multiple loops reader antenna for small size RFID LF tags," *IEEE RFID-TA*, 154–159, 2012.
5. Ahn, H. R., M. S. Kim, and Y. J. Kim, "Inductor array for minimising transfer efficiency decrease of wireless power transmission components at misalignment," *Electronics Letters*, Vol. 50, No. 5, 393–394, 2014.
6. Kim, J., H.-C. Son, and Y.-J. Park, "Multi-loop coil supporting uniform mutual inductances for free-positioning WPT," *Electronics Letters*, Vol. 49, No. 6, 417–419, 2013.
7. Diet, A., M. Grzeskowiak, Y. Le Bihan, and C. Conessa, "Improving LF reader antenna volume of detection, for RFID token tag, with a combination of ICLs and in/out-of phase multiple-loops structures," *IEEE RFID-TA*, 208–213, 2014.
8. Kawdungta, S., C. Phongcharoenpanich, and D. Torrungrueng, "Design of a novel dual loop gate antenna for radio frequency identification (RFID) systems at low frequency band," *Progress In Electromagnetics Research C*, Vol. 12, 1–14, 2010.
9. Zierhofer, C. and E. Hochmair, "Geometric approach for coupling enhancement of magnetically coupled coils," *IEEE transactions on Biomedical Engineering*, Vol. 43, No. 7, 708–714, 1996.
10. Fotopoulou, K. and B. Flynn, "Optimum antenna coil structure for inductive powering of passive RFID tags," *Proc. IEEE Int. Conf. RFID*, 71–77, 2007.
11. Azad, U., H. C. Jing, and Y. E. Wang, "Link budget and capacity performance of inductively coupled resonant loops," *IEEE Transactions on Antennas and Propagation*, 2453–2461, 2012.
12. Benelli, G., A. Pozzebon, D. Bertoni, and G. Sarti, "An RFID-based toolbox for the study of under-and outside-water movement of pebbles on coarse-grained beaches," *IEEE Journal of Selected Topics in Applied Earth Observations and Remote Sensors*, Vol. 5, No. 5, 2012.
13. Finkenzeller, K., *RFID Handbook*, 3rd edition, John Wiley & Sons, 2010.